

Unique Behavior of Dendritic Macromolecules: Intrinsic Viscosity of Polyether Dendrimers

T. H. Mourey*

Analytical Technology Division, Eastman Kodak Company,
Rochester, New York 14650-2136

S. R. Turner and Michael Rubinstein

Corporate Research Laboratories, Eastman Kodak Company,
Rochester, New York 14650-2110

J. M. J. Fréchet, C. J. Hawker, and K. L. Wooley

Department of Chemistry, Baker Laboratory, Cornell University,
Ithaca, New York 14853-1301

Received June 10, 1991; Revised Manuscript Received January 22, 1992

ABSTRACT: Polyether dendrimers made by the convergent growth approach are characterized by size exclusion chromatography (SEC) with coupled molecular weight sensitive detection. SEC chromatograms are as narrow as those of polystyrene with $M_w/M_n \approx 1.04$ and do not broaden appreciably with increasing dendrimer generation, g . Values of M_w obtained from light scattering detection are in agreement with the molecular weights of the structures anticipated from the synthetic strategy. Intrinsic viscosity, obtained from SEC viscosity detection, passes through a characteristic maximum as a function of g while the refractive index increment appears to pass through a minimum. Hydrodynamic radii, calculated from intrinsic viscosity data, increase approximately linearly with dendrimer generation. The data are in agreement with recent simulations of Lescanec and Muthukumar that predict a maximum in intrinsic viscosity as a function of g . This suggests, but does not directly prove, that the density of these dendrimers decreases monotonically from the center.

Introduction

Dendritic macromolecules are hyperbranched fractal-like structures that emanate from a central core and contain a large number of terminal groups. Two synthetic approaches have been reported for the preparation of these macromolecules: a divergent approach which is characterized by the "starburst" and "arborol" structures of Tomalia^{1,2} and Newkome,³ respectively, and more recently a "convergent growth" approach.^{4,5} The interest in these molecules is due to their globular structure, which mimics in some ways that of some naturally occurring molecules but is a result of hyperbranching rather than intermolecular interactions.

The chemical structures and fractal nature of several dendrimers have been confirmed spectroscopically; however, other properties of dendrimers that might appear to be unusual in comparison to the properties of linear synthetic polymers have been less fully investigated. In some cases, these properties differ significantly for different dendrimers. For example, a maximum in intrinsic viscosity as a function of generation has been reported for polyamidoamine (PAMAM) tridendrons made by the divergent synthesis approach.^{6,7} On the other hand, monodendrons based on lysine have intrinsic viscosities equal to 0.025 dL/g for all generations.⁸ A possible reason for this difference between these dendrimers is that they have different density profiles, depending on the length and flexibility of spacers and the interaction between monomer units.

Two theoretical models of dendritic macromolecules have been proposed recently.⁹⁻¹¹ The model developed by Lescanec and Muthukumar¹⁰ predicts a density maximum in the center of the dendrimer, while one developed by de Gennes and Hervet⁹ argues for a density minimum in the center. The predictions of other properties such as

dendrimer size and intrinsic viscosity also differ dramatically for the two models. Both models have shortcomings. The model predicting the minimum in the center of the dendrimer does not account for backfolding, which could be an incorrect assumption for flexible dendrimers. On the other hand, the model predicting the maximum in the center of the dendrimer is based on kinetically grown rather than equilibrium structures and was only simulated numerically.

The experimental situation is also unclear, in part, because viscosity data are available for only a few structurally different dendrimers.⁶⁻⁸ This paper reports the results of our characterization study of dendrimers based on benzyl ether linkages prepared by the convergent growth approach. These dendrimers are structurally different from dendrimers studied previously and have been synthesized by a different approach. An approximately linear dependence of dendrimer hydrodynamic radius on generation and a characteristic maximum in intrinsic viscosity are observed. The results are compared with data for dendrimers made by other synthetic methods and with the predictions of recent dendrimer models. These results are in quantitative agreement with the Lescanec-Muthukumar model that predicts maximum density in the center of dendrimers but do not provide direct proof for this density profile.

Experimental Section

Nomenclature. Branched structures that emanate from a single focal point such as shown in Figure 1a, based on 3,5-dihydroxybenzyl alcohol, are referred to as monodendrons. The designation [G-4]-OH describes the number of shells or generations of branch structure (in addition to the terminal groups) and the core (hydroxyl). Dendrimers obtained by coupling monodendron "wedges" to a trifunctional core, 1,1,1-tris(4'-hydroxyphenyl)ethane, are referred to as tridendrons (Figure 1b) or

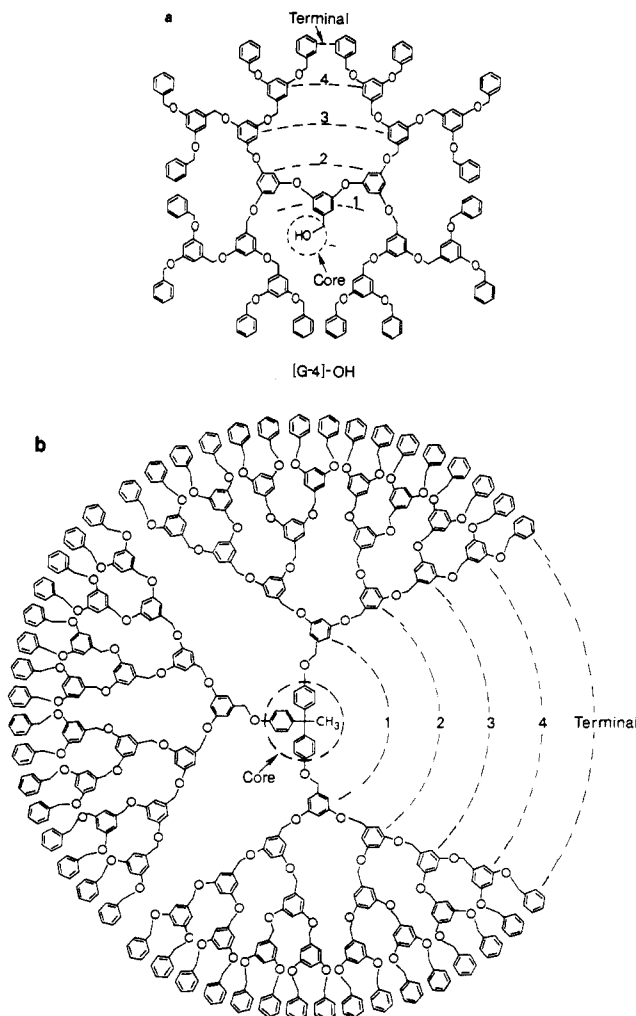


Figure 1. (a) [G-4]-OH monodendron obtained by convergent growth. (b) [G-4]₃-[C] tridendron obtained by convergent growth.

branch structures which emanate from three functional groups on a single central moiety. The accompanying designation [G-4]₃-[C] refers to three fourth-generation wedges attached to a core. The preparation, purification, and spectroscopic characterization of monodendrons and tridendrons have been described in detail previously.^{4,5}

Characterization. The SEC system using coupled low-angle laser light scattering (LALLS), differential viscometry (DV), and refractive index detection was configured as described previously.^{12,13} Four 7.5 mm i.d. × 300 mm, 10 μm particle diameter PLgel mixed-bed columns (Polymer Laboratories, Amherst, MA) were coupled in series. Uninhibited HPLC grade tetrahydrofuran (THF) (J. T. Baker), used as received, was continuously sparged with helium. Eluent was delivered at a nominal flow rate of 1.0 mL/min. The column effluent was split approximately equally to a Model 100 DV (Viscotek Corp., Porter, TX) and a LALLS photometer (LDC Analytical, Inc., Riviera Beach, FL). The DRI was attached to the outlet of the LALLS cell. The columns and the DV and DRI detectors were thermostated to 30.0 ± 1 °C.

Narrow molecular weight distribution polystyrene standards were obtained from Polymer Laboratories. Narrow standard and universal calibration curves were constructed and evaluated as described previously.¹³ Dendrimer injection concentrations ranged between 2 and 6 mg/mL for the highest and lowest molecular weight dendrimers, respectively. Injection volumes were 100 μL. Flow rates were corrected from the retention times of 1-chloro-2,4-dinitrobenzene (Kodak Laboratory Chemicals, catalog no. 101), which was added at a concentration of 0.01% (w/v) to all sample solutions and narrow standard polystyrene solutions.

Data Analysis. Unlike most conventional synthetic polymers, dendrimers made by stepwise methods can have monodisperse

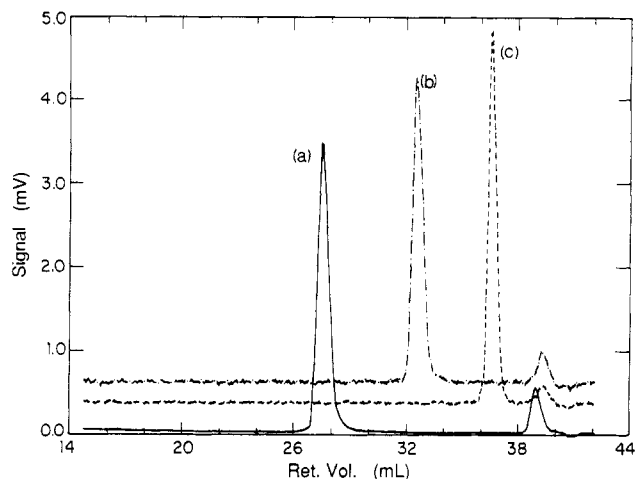


Figure 2. Size exclusion chromatogram of (a) polystyrene 155 000, $\bar{M}_w/\bar{M}_n \approx 1.04$, (b) [G-4]₃-[C] tridendron, and (c) [G-0]₃-[C] tridendron.

molecular weight distributions. Comparison of the SEC chromatograms (Figure 2) of [G-0]₃-C (MW 576) and [G-4]₃-[C] (MW 10 127) tridendrons to polystyrene with polydispersity $\bar{M}_w/\bar{M}_n \approx 1.04$ confirms that narrow molecular size distributions are obtained. However, the calculation of the absolute molecular weight distribution of these dendrimers and the true polydispersity from multidetector SEC is complicated by at least two factors. The first is a characteristic of dendrimers themselves: branched macromolecules of identical size can have different molecular weights. Thus, we can obtain only an average molecular weight of the instantaneous SEC detector cell contents, and some information on the true distribution of molecular weights is lost. The second complication is inherent to the analysis of data from multidetector SEC experiments. The eluting sample passes through each detector at slightly different times, depending on how the detectors are interconnected (e.g., in parallel, series, or a combination of both). The responses of the molecular weight sensitive (LALLS or DV) and concentration sensitive (DRI) detectors must be shifted such that they superimpose on either a time or elution volume basis. The value of the interdetector volume (the volume between detectors) required to perform the superposition is difficult to measure accurately, and incorrect values artificially broaden or narrow the absolute molecular weight distribution.¹² For narrow distributions, even an error as small as a few microliters in the interdetector volume value can result in nonsensical results, such as polydispersities less than 1.0. In addition, corrections for axial dispersion to both detector responses are necessary with narrow molecular size distributions. These corrections are sensitive to the numerical methods chosen, as well as to the values of band broadening parameters, which likewise are difficult to determine accurately.

The combination of complications to the analysis of SEC data created by having both a branched sample and a narrow size distribution is unique, and a satisfactory method for obtaining true absolute molecular weight distributions on such samples from the detectors employed here is not available. But the situation is not hopeless. We may take advantage of the separation capability of SEC to provide microquantities of sample free from monomer, solvent, and other impurities and then use LALLS and DV to measure the "whole polymer" weight-average molecular weight, \bar{M}_w , and intrinsic viscosity, $[\eta]$. These are the quantities that are normally obtained by elastic light scattering and capillary viscometry experiments on the unfractionated macromolecules, but the SEC experiment requires much less sample. The following equation is used to obtain \bar{M}_w from LALLS:

$$\bar{M}_w = \frac{1}{mK} \int_0^\infty R_\theta(v) dv \quad (1)$$

Here $R_\theta(v)$ is excess Rayleigh scattering at retention volume v , K is an optical constant which includes the polymer refractive index increment, dn/dc , and the refractive index of the solvent, and m is the total mass of sample injected. A similar expression

is used to obtain the "whole polymer" intrinsic viscosity, $[\eta]$, from DV

$$[\eta] = \frac{1}{m} \int_0^\infty \eta_{sp}(v) dv \quad (2)$$

where η_{sp} is the specific viscosity. By using eqs 1 and 2 rather than summation methods that use both the molecular weight sensitive and concentration sensitive detector signals, we maximize accuracy and precision and avoid the complications of superimposing detector responses. In addition, the calculation of $[\eta]$ and \bar{M}_w in this manner is unaffected by chromatographic resolution, thus avoiding axial dispersion corrections; however, an absolute molecular weight distribution is not obtained.

The calculation of the whole polymer \bar{M}_w from LALLS requires dn/dc of the dendrimer at 632.8 nm. Normally, dn/dc is measured in a separate instrument, which usually requires several milligrams of sample. Alternatively, it may be approximated from the DRI detector response, $G(v)$

$$\frac{dn}{dc} = \frac{k}{m} \int_0^\infty G(v) dv \quad (3)$$

where m is the total mass injected and k is a detector response factor

$$k = \frac{m_{PS}(dn/dc)_{PS}}{\int_0^\infty G(v)_{PS} dv} \quad (4)$$

obtained by integration of the DRI detector response for a compound of known dn/dc , such as polystyrene, at 632.8 nm. Although DRI detector measurements are often made at a wavelength other than 632.8 nm (the wavelength of the LALLS light source), eqs 3 and 4 approximate the value of dn/dc at this wavelength with an accuracy of approximately $\pm 3\%$, provided the polystyrene value $(dn/dc)_{PS} = 0.184$ at 632.8 nm is used. Using the approach outlined above, SEC with coupled LALLS, DV, and DRI detection provides $[\eta]$, \bar{M}_w , and dn/dc in a single experiment, requiring only an amount of sample that can be weighed accurately for a sample solution, typically a few milligrams. This is useful when sample sizes are limited, as is often the case with large dendrimers.

Results

The molecular weight of a dendrimer of generation g with core multiplicity N_c and branch-juncture multiplicity N_b can be calculated from⁶

$$M_g = M_c + N_c \left[M_{BC} \left(\frac{N_b^g - 1}{N_b - 1} \right) + M_t N_b^g \right] \quad (5)$$

where M_c , M_{BC} , and M_t are core, branch cell, and terminal unit molecular weights, respectively. The values for polyether dendrimers based on 3,5-dihydroxybenzyl units are M_c (monodendrimer) = 17, M_c (tridendron) = 303, M_{BC} (monodendrimer and tridendron) = 121, and M_t (monodendrimer and tridendron) = 91. Core multiplicities are $N_c = 1$ for monodendrimers and $N_c = 3$ for tridendrons. Branch-juncture multiplicity is $N_b = 2$ for the polyether dendrimers prepared by convergent growth. The predictions of eq 5 and the measured values of mass of monodendrimers and tridendrons synthesized by the convergent growth approach are presented in Table I. The agreement between nominal (predicted by eq 5) and weight-average molecular weights measured by LALLS of all dendrimers above 2000 MW is within the precision ($\pm 7\%$, 1σ SD) of the SEC/LALLS experiment for polymers of high dn/dc in this molecular weight range. The uncertainty in the LALLS experiment is considerably higher ($\sim \pm 20\%$) for weakly scattering dendrimers below 2000 MW. Overall, the agreement between nominal and measured molecular weights indicates that the convergent growth reactions give the structures anticipated from the synthetic strategy.

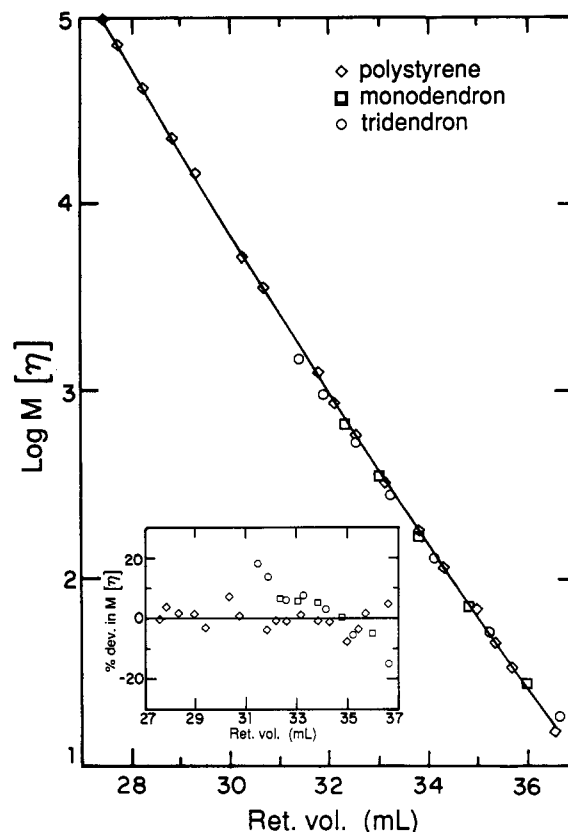


Figure 3. Universal calibration curve. (Insert) Universal calibration curve residual plot.

Table I
Convergent Growth Dendrimers

	nominal mol wt	LALLS \bar{M}_w	dn/dc , mL/g	$[\eta]$, dL/g	r_h , nm
monodendrimer					
[G-2]-OH	744	640	0.199	0.037	0.8
[G-3]-OH	1592	1800	0.201	0.045	1.0
[G-4]-OH	3288	3500	0.211	0.052	1.4
[G-5]-OH	6687	6600	0.215	0.053	1.8
[G-6]-OH	13479	14000	0.204	0.050	2.2
tridendron					
[G-0] ₃ -[C]	576	580	0.202	0.032	0.7
[G-1] ₃ -[C]	1212	1700	0.197	0.044	1.0
[G-2] ₃ -[C]	2484	2500	0.199	0.052	1.3
[G-3] ₃ -[C]	5034	5400	0.200	0.056	1.7
[G-4] ₃ -[C]	10127	10000	0.204	0.054	2.1
[G-5] ₃ -[C]	20292	20000	0.210	0.048	2.5
[G-6] ₃ -[C]	40644	38000	0.215	0.037	2.9

Comparison of a SEC universal calibration curve for polystyrene standards with that for dendrimers using the whole polymer $[\eta]$ from DV and \bar{M}_w from LALLS (Figure 3) may lead one to believe that the principle of universal calibration applies to these macromolecules. Such plots can be misleading. The assessment of fits to SEC calibration curves, and in this case the agreement of dendrimer data with the universal calibration data of Figure 3, is better accomplished through examination of residuals on a linear $[\eta]\bar{M}$ scale.¹³ Examined in this fashion (insert in Figure 3), we find that the largest dendrimers (smallest elution volumes) deviate as much as 20% from the universal calibration curve. More importantly, the pattern of residuals for the dendrimers is not randomly distributed about zero, indicating a systematic shift away from universal calibration curve with increasing g . We therefore rely on the measurement of dendrimer molecular weights by LALLS rather than viscometry detection, which requires the use of a universal calibration curve for the

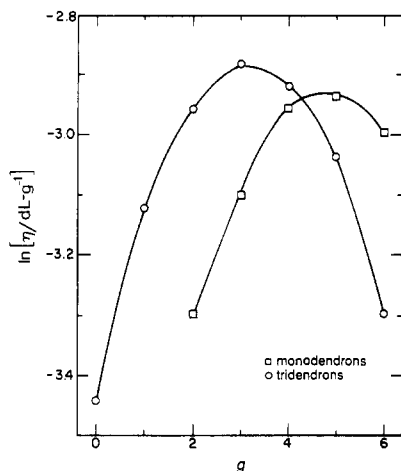


Figure 4. Intrinsic viscosity in THF of convergent growth dendrimers.

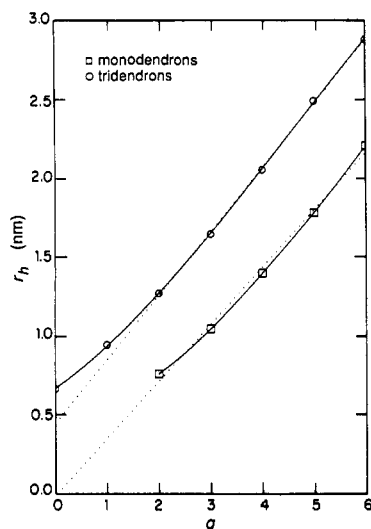


Figure 5. Hydrodynamic radii of convergent growth dendrimers as a function of generation, g . Dotted lines are linear fits to data $g = 2-6$.

calculation of molecular weights.

The intrinsic viscosity of a dendrimer can be expressed through its hydrodynamic volume, V_h , as

$$[\eta] = 2.5N_a(V_h/M) \quad (6)$$

where N_a is Avogadro's number and M is molecular weight. The intrinsic viscosity of both monodendrons and tridendrons passes through a maximum (Figure 4) as a function of generation number g . The hydrodynamic radius, r_h , can be calculated from the intrinsic viscosity using

$$r_h = [3M[\eta]/10\pi N_a]^{1/3} \quad (7)$$

Hydrodynamic radii calculated from SEC intrinsic viscosity data and eq 7 increase nearly linearly with generation number g between 2 and 6 for both monodendrons and tridendrons (Figure 5; Table I).

$$r_h = c_0 + c_1g \quad (8)$$

From Figure 5, we obtain $c_0 = 0$ nm and $c_1 = 0.36$ nm for polyether monodendrons and $c_0 = 0.44$ nm and $c_1 = 0.41$ nm for tridendrons. The maximum theoretical interspacing of a dendrimer is the fully extended length of a benzyl ether branch unit, referred to as the spacer length, S . An average value of $S = 0.6$ nm calculated from a variety of molecular modeling programs is approximately one-third larger than the experimentally measured interspacing.

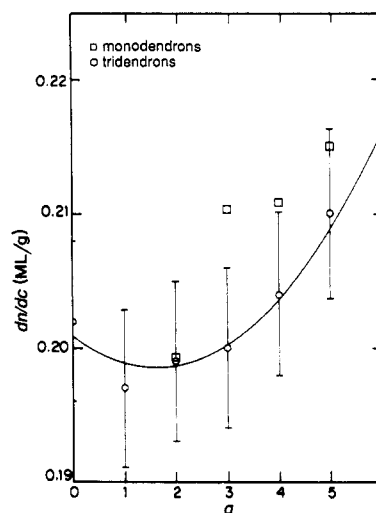


Figure 6. Refractive index increment of convergent growth dendrimers in THF. Solid line is second-order fit to tridendron data.

Thus, it appears that these dendrimers are not fully extended.

Previous authors^{1,6,14} have used the Mark-Houwink equation $[\eta] = KM^a$ (where K and a are constants specific for a polymer-solvent system) for generations 0-3. However, a compilation of all the data presented in ref 6 indicates that the dependence of $\log [\eta]$ on $\log M$ is clearly nonlinear at higher generations. No data beyond $g = 3$ were presented in ref 14. Figure 4 is actually similar to a Mark-Houwink plot because g is proportional to $\log M$. In our case the plot is even nonmonotonic. Therefore, we conclude that the application of the Mark-Houwink equation to dendrimers is inappropriate.

The average hydrodynamic density of a solvated dendrimer, defined by the reciprocal intrinsic viscosity, should have a minimum corresponding to the maximum of $[\eta]$. A minimum is therefore predicted in refractive index and refractive index increment, dn/dc , assuming that both are roughly proportional to the average dendrimer density. We lack the experimental accuracy and precision in this study to verify this prediction, but the dn/dc data in Figure 6 and the minima in both refractive index and density reported by Tomalia et al.^{6,7} for PAMAM tridendrons are consistent with the prediction.

Dendrimers Made by Other Synthetic Methods. Limited viscosity and size data have been reported for dendrimers made by other synthetic methods. The most complete set is for PAMAM tridendrons, reported by Tomalia et al.^{1,2,6,7} The radius of PAMAM dendrimers increases approximately linearly with g beyond $g = 3$. A maximum in intrinsic viscosity and minima in density and refractive index were observed between generations 4 and 5 for the PAMAM dendrimers. These results are qualitatively similar to ours for polyether dendrimers.

Monodendrons of *tert*-butoxycarbonylpoly(α , ϵ -L-lysine)s, synthesized by Denkwalter and co-workers¹⁵ and characterized by Aharoni et al.,⁸ have $r_h \sim g^{1/2}$ and a constant value for intrinsic viscosity, $[\eta] = 0.025$ dL/g, in dimethylformamide (DMF) for $g = 0-9$. The densities of all dendrimers in ref 8 are also equivalent. This indicates that volume and mass increase equally with generation, which is the limiting case $r_h \sim M^{1/3}$ for a collapsed structure. These properties distinguish these dendrimers for more extended polyether and PAMAM dendrimers.

Comparison with Existing Models. The self-consistent field model of de Gennes and Hervet⁹ assumes that

the dendrimer structure emanates radially outward from the core, with all terminal groups on the periphery of the molecule. The prediction $r \sim M^{0.2}$ of the self-consistent field calculation for dendrimers at low values of g (below the starburst limit) is not inconsistent with the approximately linear relationship of r_h and g (proportional to $\log M$) for our results; however, it predicts $[\eta] \sim M^{-0.4}$ for low generations (no maximum in $[\eta]$), while we observe an increase in $[\eta]$ at low generations (Figure 4). Molecular modeling performed by Goddard et al.^{6,16} predicts internal cavities and most of the terminal groups on the surface of large dendrimers. This is conceptually similar to the self-consistent field model of de Gennes and Hervet. Diameters of PAMAM dendrimers were calculated for various generations and compared to hydrodynamic sizes calculated both from SEC data via universal calibration (which we have shown may not be valid for all dendrimers) and from intrinsic viscosity measurements. The application of eq 6 to the sizes predicted from modeling indicates that most of the calculated diameters do not provide good estimates of intrinsic viscosity. Of several simulation methods, diameters calculated from the solvent-accessible surface (V_{SAS}) method predict a maximum in intrinsic viscosity as a function of generation, although some predicted values are as much as 45% greater than experimental quantities. Diameters calculated by other means in refs 6 and 16 either do not predict a maximum in $[\eta]$ or grossly overestimate the experimental values of $[\eta]$.

A model developed by Lescanec and Muthukumar¹⁰ predicts inward folding of branch units, a density maximum in the center, and a distribution of terminal groups throughout the structure. The model is based on a self-avoiding walk algorithm that simulates kinetic growth of dendrimers. It also predicts an approximately linear relationship between r and g over a narrow range of g . In addition, a maximum in $[\eta]$ is predicted with $[\eta] \sim M^{0.5}$ at small g and $[\eta] \sim M^{-0.4}$ at large g . Klushin and Mansfield¹¹ calculated upper and lower limits of reduced hydrodynamic radii, defined as r_h/S , of the Lescanec-Muthukumar model using intrinsic viscosity formulas developed by Zimm¹⁷ and Fixman.¹⁸ These quantities can be compared directly with our results after two differences between the Klushin and Mansfield versions of the self-avoiding walk model and polyether dendrimers are accounted for. First, this model begins counting generations at 1, while our convention is to begin counting generations at 0; therefore, the [G-4]-[C] dendrimer of Figure 1b is generation $g + 1 = 5$ by the Klushin and Mansfield (Lescanec-Muthukumar) convention. Second, the model assumes a string of beads, all with diameter of 1.0 and spacer length of 1.2. It does not provide for a core that is larger than the branch beads, as is the case for polyether dendrimers. The calculated value of $S = 0.6$ nm is half the value of the spacer length of the simulation (1.2 in arbitrary units); thus, we estimate the "bead" radius of the polyether branch units to be half the radius of the simulation bead, or 0.25 nm. The radius of the polyether dendrimer core is approximately 0.46 nm. The difference between the core structures is accounted for in the model as twice the difference between the polyether core and bead radii, or $2 \times (0.46 - 0.25) = 0.42$. This value is added to each hydrodynamic radius listed in ref 11. After this accounting for the core of polyether dendrimers, the upper and lower limits for reduced hydrodynamic radii calculated for one spacer (step) between branch sites in the model are in good agreement with our data (Figure 7). The best fit to PAMAM reduced radii was obtained for a model

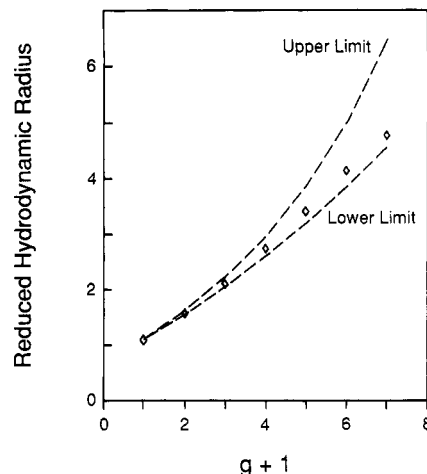


Figure 7. Reduced hydrodynamic radii of convergent growth dendrimers. Dashed lines are upper and lower limit predictions of ref 11 shifted by 0.42 for one-step spacer, as described in the text.

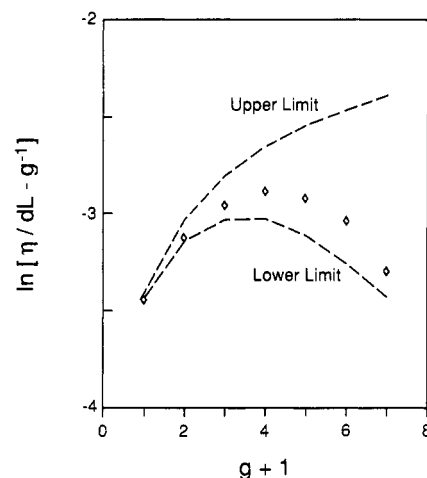


Figure 8. Intrinsic viscosity of convergent growth dendrimers. Dashed lines are upper and lower limits calculated from radii of ref 11 shifted by 0.42 for one-step spacer and molecular weights of polyether dendrimers.

with two spacers between branch sites in ref 11. This is consistent with PAMAM structures being less rigid than the polyether dendrimers of this study. Upper and lower limit predictions of intrinsic viscosity (Figure 8) are obtained by substituting ref 11 values $R_h + 0.42$ and nominal molecular weights of polyether dendrimers (Table I) into rearranged eq 7. The lower limit approximation properly predicts the maximum in $[\eta]$, and the upper and lower limits bracket the data (Figure 8).

Agreement of our data with predictions for radii and intrinsic viscosity strongly supports, but is not direct proof of, the Lescanec-Muthukumar model. If there are no specific interactions between groups and if the branch units of the dendrimer are flexible enough to allow some gradual backfolding, it is reasonable that the equilibrium structure has maximum density in the center because this corresponds to maximum entropy for the molecule and also provides relief of steric crowding of terminal groups. An analytical mean-field calculation of this structure supports this picture.¹⁹ It is also significant that this model describes the intrinsic viscosity behavior of both PAMAM¹¹ and polyether dendrimers; this implies that the model describes properties general to all flexible dendritic macromolecules.

There still remain unanswered questions, however, about the true radial distribution of terminal groups and the

density distribution that cannot be answered unambiguously from whole polymer properties such as intrinsic viscosity. These questions emphasize the need for further experimental (e.g., scattering) and numerical work to model these structures and to resolve the theoretical controversy.

Conclusions

Size exclusion chromatography with coupled molecular weight sensitive detection is a simple, convenient method for characterizing dendrimers for which limited sample quantities are available. The calculation of whole polymer quantities from the molecular weight sensitive detector responses is the key to the elimination of a variety of data analysis complications that are specific to narrow dendrimer size distributions. The polyether dendrimers increase in hydrodynamic radius approximately linearly with generation and have a characteristic maximum in viscosity. These properties distinguish these dendrimers from completely collapsed, globular structures. The experimental data also indicate that these structures are extended to approximately two-thirds of the theoretical, fully extended length. Of the existing models for dendrimer structures, simulations of Lescanec and Muthukumar¹⁰ and Klushin and Mansfield¹¹ most closely predict the experimentally measured radii and intrinsic viscosities of polyether dendrimers; however, additional experiments are needed to test in detail other properties (i.e., radial density distribution).

Acknowledgment. We thank Sally Miller for her laboratory assistance and Hans Coll, Dennis Massa, and Hyuk Yu for valuable comments. Financial support by the National Science Foundation (DMR 8913278) is

acknowledged.

References and Notes

- (1) Tomalia, D. A.; Baker, H.; Dewald, J.; Hall, M.; Martin, S.; Roeck, J.; Ryder, J.; Smith, P. *Polym. J.* **1985**, *17*, 117.
- (2) Tomalia, D. A.; Baker, H.; Dewald, J.; Hall, M.; Kallos, G.; Martin, S.; Roeck, J.; Ryder, J.; Smith, P. *Macromolecules* **1986**, *19*, 2466.
- (3) Newkome, G. R.; Yao, Z.; Baker, G. R.; Gupta, V. K. *J. Org. Chem.* **1985**, *50*, 2004.
- (4) Hawker, C. J.; Fréchet, J. M. J. *J. Chem. Soc., Chem. Commun.* **1990**, *15*, 1010.
- (5) Hawker, C. J.; Fréchet, J. M. J. *J. Am. Chem. Soc.* **1990**, *112*, 7638.
- (6) Tomalia, D. A.; Naylor, A. M.; Goddard, W. A., III. *Angew. Chem., Int. Ed. Engl.* **1990**, *29*, 138.
- (7) Tomalia, D. A.; Hedstrand, D. M.; Wilson, L. R. In *Encyclopedia of Polymer Science and Engineering*, 2nd ed.; Wiley: New York, 1990; Index, pp 69–75.
- (8) Aharoni, S. M.; Crosby, C. R., III; Walsh, E. K. *Macromolecules* **1982**, *15*, 1093.
- (9) de Gennes, P.-G.; Hervet, H. *J. Phys. Lett.* **1983**, *44*, L-351.
- (10) Lescanec, R. L.; Muthukumar, M. *Macromolecules* **1990**, *23*, 2280.
- (11) Klushin, L. I.; Mansfield, M. L. *J. Phys. Chem.* **1992**, in press.
- (12) Mourey, T. H.; Miller, S. M. *J. Liq. Chromatogr.* **1990**, *13*, 693.
- (13) Mourey, T. H.; Miller, S. M.; Balke, S. T. *J. Liq. Chromatogr.* **1990**, *13*, 435.
- (14) Morikawa, A.; Kakimoto, M.; Imai, Y. *Macromolecules* **1991**, *24*, 3469.
- (15) Denkwalter, R. G.; Kolc, J. F.; Lukasavage, U.S. Pat. 4410688, 1983; *Chem. Abstr.* **1984**, *100*, 103907p.
- (16) Naylor, A. M.; Goddard, W. A., III; Keifer, G. E.; Tomalia, D. A. *J. Am. Chem. Soc.* **1989**, *111*, 2339.
- (17) Zimm, B. H. *Macromolecules* **1980**, *13*, 592.
- (18) Fixman, M. *J. Chem. Phys.* **1983**, *78*, 1588.
- (19) Boris, D.; Rubinstein, M. Unpublished results.

Registry No. [G-4]-OH (homopolymer), 106903-39-3.